Electronic Supplementary Information for: Slip and momentum transfer mechanisms mediated by Janus rods at polymer interfaces

Felipe L. Paiva,[a,b] Argimiro R. Secchi,[c] Verônica Calado,[a] João Maia,*[,b] and Shaghayegh Khani*[,b]

1 Bare interface and polymer chain end concentration

Fitted density profiles as explained in the main text are illustrated in Figure S1a. Furthermore, polymer chain ends are expected to be intrinsically associated with higher conformational entropy and MD results from Barsky and Robbins [1] indicated that they preferably located at the interface to minimize unfavorable interactions of adjacent monomers. The normalized relative abundance of chain ends $R(y) = \frac{\phi^{CE}_{A,B}(y)}{\left(\frac{2}{C}\right)}$ can be calculated,[1,2] where $\phi^{CE}_{A,B}(y)$ is the local fraction of chain ends (CE) at a given distance from the interface $\left(\phi^{CE}_{A,B}(y) = \frac{\rho^{CE}_{A,B}(y)}{\rho}\right)$. However, contrary to MD results from Barsky and Robbins [1], chain ends do not tend to concentrate at the interface (Figure S1b). This may be due to (i) the soft potentials and possibility of bond crossing events in DPD;[3] (ii) a loss of sufficient resolution and detail in DPD in view of coarse-graining; (iii) and/or polymers may be simply still not long enough to observe this behavior. Guo *et al.*[4] argued using DPD that, in a similar polymer system, interfacial polymers are easier to deform than bulk polymers because of the extra repulsion at the interface. Even though this reasoning agrees with discussions made by Barsky and Robbins [1], Guo *et al.*[4] did not assess neither the proportion of chain ends at the interface nor interfacial slip. In any case, the present DPD model captures several previously-observed trends with other simulation techniques,[1,5,6] including slip, momentum transfer, and those related with a_I, S, and η_I (Figures 2 and 4 in the main text).

2 Interfacial slip at bare interfaces

Average particle velocities for each polymer component ($V_{x,A}(y)$; $V_{x,B}(y)$) are shown separately in Figures S2a and S2b and illustrate how sharp the interface is. Zero velocity values in separate halves of Figures S2a and S2b are encountered because no particles for the corresponding component have been detected.

A slip length S is calculated fitting velocity profiles (Figure S2c) to obtain a bulk shear rate and extrapolated upper and lower velocities at the interface: V_x^U and V_x^L respectively. The slip length is then simply $S = \frac{\Delta V}{\dot{\gamma}_B}$, where $\Delta V = V_x^U - V_x^L$ and an average bulk shear rate $\dot{\gamma}_B$ is considered based on upper and lower fitted shear rates ($\dot{\gamma}_B^U$ and $\dot{\gamma}_B^L$ respectively). Much like a_I (Figure 2 in the main text), these parameters change only slightly as a function of χ and C (FIgure S2d,e,f,g). More notably, they seem to be more dependent on C for the highest χ only.

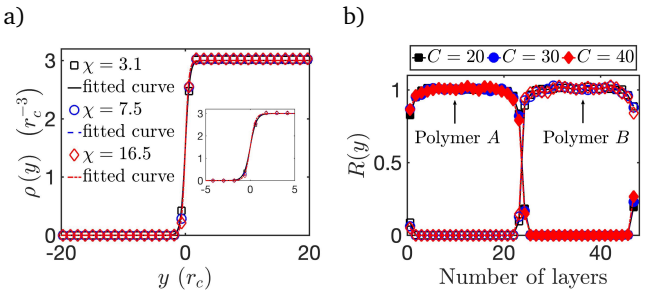

Fig. S1 a) Fitted density profiles for polymer B (Equation 10 in the main text), where the domain is [-20 20] and the inset is simply an augmented region ($C = 20$); b) relative abundance of chain ends across the interface as a function of C ($\chi = 16.5$) where filled symbols correspond to polymer A and empty symbols to polymer B.

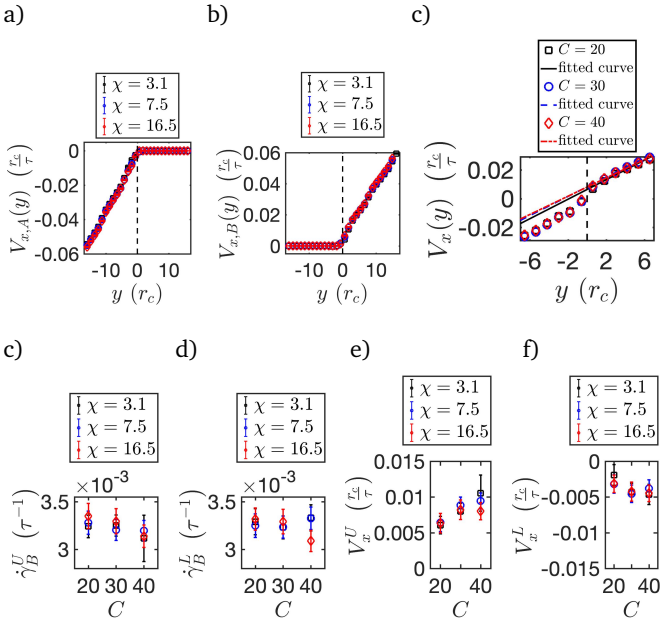

Fig. S2 Average velocity profiles separately for each component as a function of χ: a) polymer A; b) polymer B; and c) fitted velocity profiles ($\chi = 16.5$) where the domain for the fitting is taken to be either [-17 -2] or [2 17] to finally obtain a slip length. The domain for calculating interfacial viscosities of bare interfaces (Figure 4a in the main text) is accordingly [-2 2]; c) upper and d) lower fitted bulk shear rates; e) upper and f) lower extrapolated velocities at $y = 0$. Error bars in c); d); e); and f) are based on 95% confidence intervals from the fittings. Error bars in a) and b) plots are based on standard deviation calculations. The dashed lines at $y = 0$ in c) indicate where the interface is initially generated in the simulations.

[a] *School of Chemistry, Universidade Federal do Rio de Janeiro, Rua Horácio Macedo 2030, Cidade Universitária, Rio de Janeiro, RJ 21941-909, Brazil.*
[b] *Department of Macromolecular Science and Engineering, Case Western Reserve University, 2100 Adelbert Road, Cleveland, OH 44106, USA.*
[c] *Chemical Engineering Graduate Program (COPPE), Universidade Federal do Rio de Janeiro, Rua Horácio Macedo 2030, Cidade Universitária, Rio de Janeiro, RJ 21941-909, Brazil.*
* *E-mail: joao.maia@case.edu; shaghayegh.khani@case.edu.*

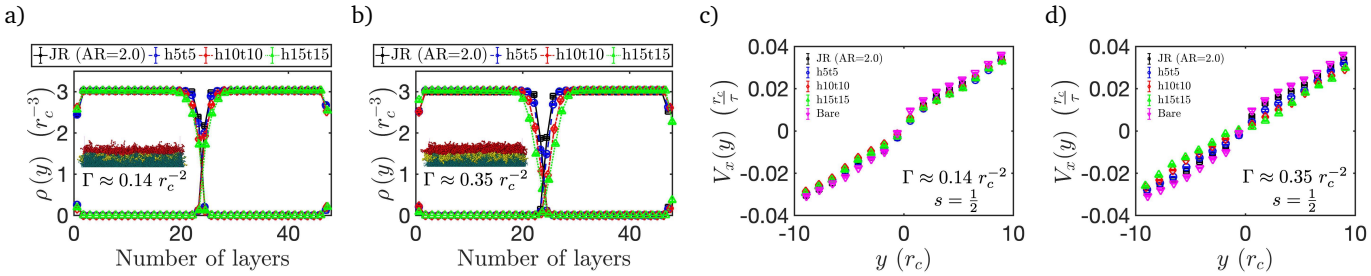

Fig. S3 Density profiles for polymer A and polymer B as a function of compatibilizer type and for different interfacial concentrations ($\chi = 16.5$; $C = 40$): a) $\Gamma \approx 0.14\ r_c^{-2}$; b) $\Gamma \approx 0.35\ r_c^{-2}$. Insets are corresponding simulation snapshots of the interface (h15t15); and velocity profiles in the flow direction as a function of compatibilizer type with $s = \frac{1}{2}$: c) $\Gamma \approx 0.14\ r_c^{-2}$; d) $\Gamma \approx 0.35\ r_c^{-2}$. Red and yellow DPD particles in the insets of a) and b) represent the different portions of the h15t15 surfactant molecule.

3 Polymer-polymer interfaces with flexible and rigid compatibilizers

The fact that the interfacial region becomes more diffuse for longer compatibilizers, as well as how this varies with concentration, is depicted in Figure S3. Results are shown for $\chi = 16.5$ and $C = 40$ in Figure S3 even though they apply to the entire parameter space analyzed herein.

Velocities corresponding to the set shear rate are applied by lower/upper boxes moving in opposite directions with respect to the actual calculation box using periodic boundary conditions in all directions.[7] Sufficiently-long diblock copolymers contribute to less effective momentum transfer across the interface. This can be seen in Figure S3c,d for the modified weight functions of $\mathbf{F_{ij}^R}$ and $\mathbf{F_{ij}^D}$. According to the expression used by Fan *et al.*[8], the Schmidt number Sc can be estimated to be 7 times higher when $s = \frac{1}{2}$ for the parameters utilized herein. The fact that this behavior has been observed with other techniques[4–6] reinforces how physically meaningful it is even if DPD is intrinsically associated with lower Sc.

The orientation degree of compatibilizers can be measured from the angle θ that they make during flow with the x direction in the form of $\langle \cos^2 \theta \rangle$. The orientation of compatibilizers is inversely correlated with how efficiently momentum is transferred (Figure S3c,d) from results presented in Figure S4.

4 Polymer-grafted Janus rods

The two-dimensional (2D) diffusion coefficient of various compatibilizers has been measured: $D_{2D} = lim_{t\to\infty}\left(\frac{1}{4}\frac{MSD}{\Delta t}\right)$, where MSD stands for the mean square displacement ($MSD = \langle \Delta r^2(t) \rangle$) of surfactant particles and, for Janus rods (JRs), it is measured based on their center of mass. Janus rods diffuse much more slowly than diblock copolymers because of aggregation and, overall, larger compatibilizers diffuse slower than larger ones, as would be expected (Figure S5). The red dashed square in Figure S5 illustrates how the center of the rigid portion of polymer-grafted JRs always diffuses faster than its graft-free counterpart (Figure 8b in the main text). This is due to aggregate disruption as discussed in the main text.

Simulation snapshots looking down in the y direction exemplify the homogeneous/random distribution of flexible diblock copolymers at the interface between polymers (Figure S6). It is possible

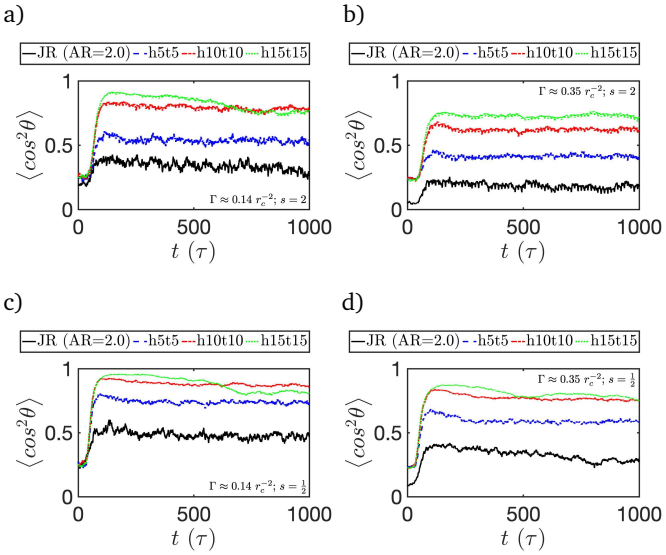

Fig. S4 Ensemble mean orientation of compatibilizers in the flow direction during shear flow for different interfacial concentrations Γ ($\chi = 16.5$; $C = 40$) using standard DPD parameters ($s = 2$): a) $\Gamma \approx 0.14\ r_c^{-2}$; b) $\Gamma \approx 0.35\ r_c^{-2}$; and using modified weight functions $\left(s = \frac{1}{2}\right)$ to raise Sc: c) $\Gamma \approx 0.14\ r_c^{-2}$; d) $\Gamma \approx 0.35\ r_c^{-2}$.

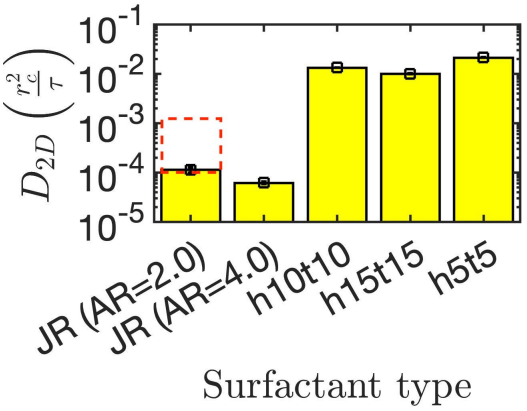

Fig. S5 Ensemble mean D_{2D} from equilibrium simulations according to surfactant type. The red dashed square denotes the region in which D_{2D} values for polymer-grafted JRs are (Figure 8b in the main text), as calculated taking into account only the center of mass of the rigid portion of JRs. Error bars are based on standard deviation calculations.

to take advantage of nanoparticle aggregation to control/tune 2D interfacial nanostructure through the number of polymer grafts N_g and their length L_g (Figure 9 in the main text).

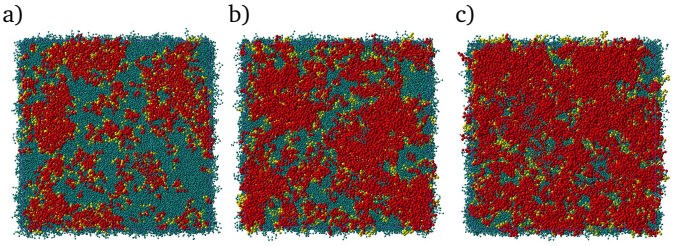

Fig. S6 Simulation snapshots for a) h5t5; b) h10t10; and c) h15t15.

Shear stress transients $\sigma_{xy}(t)$ reveal little difference in the ensemble mean steady-state shear stress among the various compatibilizers (Figure S7a). No stress overshoots have been verified. Depending on compatibilizer type/architecture and their stress contributions, shear stresses at the interface may differ slightly (Figure S7b). Ensemble mean or bulk steady-state stresses are used to extract ξ_{xx}.[5,6] To show how stress dips at the interface do not affect conclusions pertaining to ξ_{xx}, an interfacial viscosity η_I has been separately calculated in the form of a Boussinesq number[9] Bo ($Bo = \frac{\eta_I}{\eta h}$) from shear rates/stresses specifically at the interface. The domain for calculating interfacial shear rates, stresses, and thus η_I was $-2 \leq y \leq 2$, similarly to slip studies in Figure S2. Additionally, they do not vary significantly if this interval is increased. This interval is also justified by calculated h values in the main text. The strong correlation between ξ_{xx} and Bo (Figure 11 in the main text) elucidates how higher Bo allows for less efficient momentum transfer across polymer-polymer interfaces. A particle Stokes number St has also been calculated to illustrate how inertial forces are negligible compared to viscous forces:[10] $St = \frac{m_p \dot{\gamma}}{6\pi\eta a}$; where m_p is the particle mass, and a is a characteristic particle size taken to be h.[10] For all compatiblizers, $St = \mathcal{O}(10^{-5})$, whether interfacial or bulk shear viscosities/rates are considered.

a)

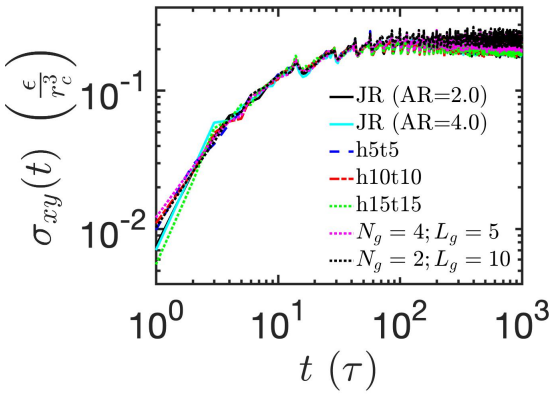

b)

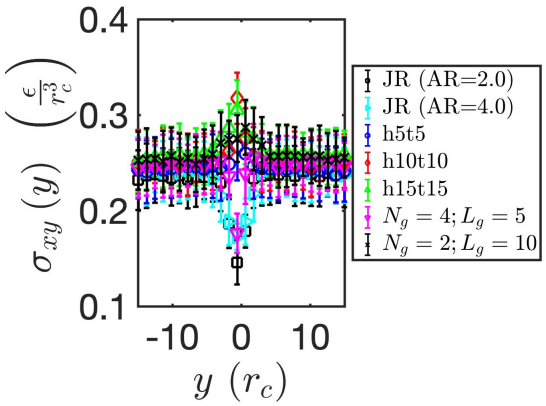

Fig. S7 a) Time evolution of the ensemble mean shear stress σ_{xy} as a function of surfactant type/architecture; and b) shear stress profiles (time averaged) across the interface as a function of surfactant type/architecture. Error bars in b) denote standard deviation calculations.

References

1 S. Barsky and M. O. Robbins, *Physical Review E - Statistical, Nonlinear, and Soft Matter Physics*, 2001, **63**, 1–7.

2 E. Helfand, S. M. Bhattacharjee and G. H. Fredrickson, *The Journal of Chemical Physics*, 1989, **91**, 7200–7208.

3 N. A. Spenley, *Europhysics Letters (EPL)*, 2000, **49**, 534–540.

4 R. Guo, J. Li, L.-T. Yan and X.-M. Xie, *Soft Matter*, 2013, **9**, 255–260.

5 L. M. C. Sagis, B. Liu, Y. Li, J. Essers, J. Yang, A. Moghimikheirabadi, E. Hinderink, C. Berton-Carabin and K. Schroen, *Scientific Reports*, 2019, **9**, 2938.

6 B. Narayanan, V. A. Pryamitsyn and V. Ganesan, *Macromolecules*, 2004, **37**, 10180–10194.

7 A. W. Lees and S. F. Edwards, *Journal of Physics C: Solid State Physics*, 1972, **5**, 1921–1928.

8 X. Fan, N. Phan-Thien, S. Chen, X. Wu and T. Yong Ng, *Physics of Fluids*, 2006, **18**, 063102.

9 G. G. Fuller and J. Vermant, *Annual Review of Chemical and Biomolecular Engineering*, 2012, **3**, 519–543.

10 J. Mewis and N. J. Wagner, *Colloidal Suspension Rheology*, Cambridge University Press, 2012.